NTIS HC #3.50

X-645-73-34

NASA TM X- 66172

A MAGNETOSPHERIC FIELD MODEL INCORPORATING THE OGO 3 AND 5 MAGNETIC FIELD OBSERVATIONS

MASAHISA SUGIURA
D. J. POROS

JANUARY 1973

GSFC

GODDARD SPACE FLIGHT CENTER
GREENBELT, MARYLAND

A MAGNETOSPHERIC FIELD MODEL INCORPORATING THE OGO 3 AND 5 MAGNETIC FIELD OBSERVATIONS

MASAHISA SUGIURA
Laboratory for Space Physics
Goddard Space Flight Center, Greenbelt, Maryland 20771

D. J. POROS
Computer Science Corporation
Silver Spring, Maryland 20910

January 1973

工

ABSTRACT

A magnetospheric field model is presented in which the usually assumed toroidal ring current is replaced by a circular disk current of finite thickness that extends from the tail to geocentric distances less than 3 R_E. The drastic departure of this model from the concept of the conventional ring current lies in that the current is continuous from the tail to the inner magnetosphere. This conceptual change was required to account for the recent results of analysis of the OGO 3 and 5 magnetic field observations. In the present model the cross-tail current flows along circular arcs concentric with the earth and completes circuit via surface currents on the magnetopause. Apart from these return currents in the tail magnetopause, Mead's (1964) model is used for the field from the magnetopause current. The difference scalar field, ΔB, defined as the difference between the scalar field calculated from the present model and the magnitude of the dipole field is found to be in gross agreement with the observed ΔB (i.e., the observed scalar field minus a scalar reference geomagnetic field). An updated version of the ΔB contours from the OGO 3 and 5 observations, which is used for the comparison, is presented in this paper. Significant differences in details exist, however, between the model and the observed results. These differences will provide a guide for making modifications in the equatorial current system in future models.

1. Introduction

Several magnetospheric field models have been proposed and are currently in use (e.g., Mead, 1964; Williams and Mead, 1965; Fairfield, 1968; Olson, 1969). However, recent analyses of the magnetic field observations on the OGO 3 and 5 satellites have shown features that are substantially different from the existing magnetospheric models (Sugiura et al., 1971; Sugiura, 1972a, 1972b). Two important conclusions were drawn from these studies. First, the field depressions in the inner magnetosphere must be caused by an equatorial current sheet which extends from the tail to geocentric distances of about 3 R_E or less. Secondly, there is a $+\Delta B$ region at middle to high latitudes in the nightside magnetosphere. The purpose of the present paper is to show that gross features of these aspects can be represented by a model that includes a magnetopause current, a neutral sheet current, and a disk current of which the intensity is uniform from the inner edge of the neutral sheet current to 3 R_E and then decreases inward to zero at 2 R_E.

Two significant features are incorporated in this model; they are (a) return currents of the neutral sheet current via the magnetopause surface and (b) the equatorial current sheet which replaces the usual toroidal ring current. The point (a) was taken into consideration in the model presented by Schield (1969). In the model described below, the neutral sheet current flows along circular arcs concentric with the earth so that the circular sheet current representing the ring current continues from the tail current without any discontinuity. The current density in the near-earth tail estimated by Speiser and Ness (1967) shows such a circular pattern rather than the usually

assumed rectilinear sheet current flowing perpendicular to the earth-sun line.

The model is not a physical one in two respects. First, the magnetopause current is represented by the Mead (1964) model, and hence is self-consistent only with the dipole field and not with the combined field of the dipole, the tail current, and the ring current. Secondly, the ring current is not based on any particle distribution. Regarding the first point, it does not seem advisable to make the elaborate calculations required for the determination of the boundary current until we have a reasonably good model for other sources. Besides, the effect of the magnetopause current is secondary to the ring current effect in the context of the present discussion. As to the second question, the intent of this paper is to give a first order approximation which would provide a guide for future studies.

2. Magnetospheric Field Model

The earth's main field. This is represented by a dipole field with an equatorial surface field of 0.31 gauss (1 gauss = 10^{-4} tesla; the unit of gamma is used below, where $1\gamma = 10^{-9}$ tesla). The dipole axis is perpendicular to the earth-sun line in the present model.

The magnetopause current. The magnetic field from the magnetopause current is represented by the spherical harmonic expansion of the scalar potential given by Mead (1964); the coefficients up to m = 5, n = 6 in his Table 1 are used. The distance, r_b, from the center of the earth to the boundary along the earth-sun line is taken to be 10 R_E.

The tail current. To describe the tail current we use the (geocentric) solar geomagnetic coordinate system, i.e. the x-axis toward

the sun, the +z-axis along the dipole axis and toward the north dipole pole, and the y-axis completing a right-handed system. The tail current consists of two parts: (a) an equatorial cross-tail current and (b) return currents flowing on the northern and southern magnetopause surface (Fig. 1). The cross-tail current flows parallel to the xy plane between $z = \pm z_1$ so that its thickness is $2z_1$. On any plane parallel to the xy plane and within this range of z, the current density $\underline{j}(j_x, j_y)$ is expressed by a current function $\Psi(x,y)$ such that

$$j_x = \partial\Psi/\partial y, \text{ and } j_y = -\partial\Psi/\partial x \tag{1}$$

Then $\nabla.\underline{j} = 0$ is automatically satisfied, and lines of equal Ψ are current-flow lines. Currents flow along ellipses of the same eccentricity, e, if Ψ satisfies

$$(1-e^2)\ (y/x)\ \partial\Psi/\partial x - \partial\Psi/\partial y = 0 \tag{2}$$

In the model, circular currents are assumed, but the formulas are given below for a more general elliptical flow pattern, from which circular currents can be obtained by putting e = 0.

If j_y is specified along the x-axis (actually the - x-axis for the tail) by

$$j_y(x,0) = -\ (\partial\Psi/\partial x)_{x,y\,=\,0} = f(x) \tag{3}$$

then Ψ along the x-axis is given by

$$\Psi(x,0) = -\int_{x_1}^{x} f(x)dx + \Psi_1 \tag{4}$$

where x_1 is the position of the earthward edge of the cross-tail current, and Ψ_1 is a constant. Equation (4) provides the boundary condition for (2).

Obviously, any function of $x^2 + (1-e^2)\, y^2$ ($\equiv a^2$) satisfies (2), because a^2 is a constant of an ellipse, $\underline{a}$ being the semi-axis along the x-axis. When f(x) is constant, i.e. when the tail current density along the x-axis is independent of x, say f(x) = C, then the functional form of $\Psi(a^2)$ can be readily determined:

$$\Psi = -C\,[x^2 + (1-e^2)\, y^2]^{\frac{1}{2}} \tag{5}$$

Now, we take C to be a function of z to give a finite thickness to the cross-tail current. Then j_x, j_y and the total current density j ($= [j_x^2 + j_y^2]^{\frac{1}{2}}$) are given by

$$j_x = -\, C(z)\, (1-e^2)\, y\,[x^2 + (1-e^2)\, y^2]^{-\frac{1}{2}} \tag{6}$$

$$j_y = C(z)\, x\,[x^2 + (1-e^2)y^2]^{-\frac{1}{2}} \tag{7}$$

$$j = C(z)\, \{[x^2+(1-e^2)^2 y^2] \,/\, [x^2+(1-e^2)y^2]\}^{\frac{1}{2}} \tag{8}$$

On the boundary, j(z) is obtained from (8) by putting $y = \pm D$ (Fig. 1). To make the current divergence-free on the boundary surface the magnitude of the surface current $J_s(z)$ for $-z_1 \le z \le z_1$ is taken to be

$$J_s(z) = \left| \int_0^z j(z;\, y = \pm D)\, dz \right| \tag{9}$$

For $z < -z_1$ and $z > z_1$, the boundary is a cylindrical surface of radius $(D^2 + z_1^2)^{\frac{1}{2}}$, and $J_s(z) = \text{const} = J_s(z_1)$.

We assume the following form for C(z):

$$C(z) = K \cos^2 (\pi z/2z_1) \tag{10}$$

where K is a constant. Thus C(z) = 0 at $z = \pm z_1$, that is, the current diminishes to zero at these values of z; z_1 is taken to be 2 R_E in the model. With (10) for C(z), (9) reduces to

$$J_s(z) = \frac{Kz_1}{2\pi} \left(\frac{\pi z}{z_1} + \sin \frac{\pi z}{z_1}\right) \left\{ [x^2+(1-e^2)^2D^2]/[x^2 + (1-e^2)D^2] \right\}^{\frac{1}{2}} \tag{11}$$

The tail current extends from x = -10 to -40 R_E in the present model. The magnetic field from the tail current is then obtained by the Biot-Savart law through integration over all the currents. This also applies to the field from the ring current described below. The constant K was chosen such that the field from the tail current is 30γ at x = -20 R_E, y = 0, and z = 5 R_E, i.e., just above the current slab.

The ring current. The ring current is represented by a current disk having the same thickness, $2z_1$, as the cross-tail current. The outer radius of the disk equals $|x_1|$ so that the disk is in contact with the cross-tail current slab on the night side. The thickness is uniform from the outer edge, taken to be 10 R_E, to 3 R_E, and inside the latter distance it decreases linearly, and symmetrically with respect to the equator, to become zero at 2 R_E. In the disk, the current is circular and concentric with the earth; the current density, which is independent of radial distance, varies with z (for $-z_1 \leq z \leq z_1$) in the same manner as in the tail so that there is no discontinuity in the current density at the interface between the disk current and the cross-tail current. In expressing the current density, a current

function of the same type as for the tail, with e = 0, is used.

3. Discussions

It has been demonstrated that the topology of ΔB is a useful concept in the analysis of magnetic field observations in the magnetosphere (Sugiura, 1972a). Here, ΔB is the observed scalar field minus a scalar reference field. The latest version of contour maps of equal ΔB determined from the OGO 3 and 5 observations for the noon-midnight and dawn-dusk meridians for quiet (Kp = 0-1) and slightly disturbed (Kp = 2-3) conditions is presented in Figures 2 through 5. Equal ΔB contours provide a simple, but rather sensitive means of quantitatively comparing magnetospheric field models with observations.

Figures 6 and 7 show ΔB contours, respectively in the noon-midnight and dawn-dusk meridians, determined from the model described in the preceding section. A comparison of Figures 2 and 6 for the noon-midnight meridian indicates a remarkable similarity in general character. The agreement between the observed results and the model is striking when compared with the ΔB contours for the Mead-Williams model (without a ring current) and those for the Hoffman-Bracken model of a ring current (incorporated in the Mead-Williams model), which were shown by Sugiura et al. (1971). However, there are significant differences between the contours in Figures 2 and 6 in the following respects. (i) Magnitudes of the field depressions near the equator at close distances ($\lesssim 4\ R_E$) are smaller in the model than in the observed results. This is especially conspicuous for noon. (ii) $+\Delta B$ at middle latitudes on the nightside is greater in the model than the observed. (iii) The magnitudes of $-\Delta B$ at high latitudes in the noon

meridian are substantially larger in the model than the observed. (iv) The $+\Delta B$ values in the outer region of the equatorial magnetosphere are slightly larger in the model than those in the observed.

The nighttime, middle-latitude $+\Delta B$ in Figure 6 is more like that in Figure 4 for Kp = 2-3, but then the equatorial $-\Delta B$ values in Figure 6 are more different from Figure 4 than from Figure 2. Magnitudes of the daytime, high-latitude $-\Delta B$ in Figure 6 are even greater than the corresponding values in Figure 4 for slightly disturbed conditions. Thus a simple intensification or reduction of the disk current would not result in a better agreement between the model and the observations.

A comparison of Figures 7 and 3 (or 5) for the dawn-dusk meridian shows differences that are consistent with those for the noon meridian. The main differences lie in: (i) smaller magnitudes of the equatorial $-\Delta B$ in the model than the observed, and (ii) the existence of a large $-\Delta B$ region over the pole in the model. Though the data coverage is not complete, the observed ΔB over the northern polar cap is probably only slightly negative beyond the geocentric distance of about 7 or 8 R_E for the Kp = 0-1 condition (Figs. 2 and 3), and is all positive for Kp = 2-3 (Figs. 4 and 5).

The differences between the ΔB distributions from the model and the observations described above appear to imply (a) that the equatorial ring (or disk) current in the model is too weak in the inner magnetosphere especially on the dayside, and (b) that the observed fields at high latitudes on the dayside and over the polar cap are not well represented by the model. It is noted that the present model for the ring current does not include the eastward current due to the pressure

gradient at the inner edge of the particle disk, and hence that the deficiency in the field depressions in the innermost magnetosphere is actually greater than is apparent in the above comparison if the effect of the eastward current is taken into account. The existence of indentations in the ΔB contours in Figure 6 in the outer region of the dayside equatorial magnetosphere may imply that the particle disk is thicker and less concentrated near the equator than in the model in this region. Whether or not the magnitudes of $-\Delta B$ at high latitudes on the dayside and over the pole can be reduced sufficiently to match the observed values by increasing the ring current intensity is not obvious. But it seems unlikely that the very large $-\Delta B$ ($\sim -40\gamma$) near the magnetopause can be reduced substantially by altering the ring current intensity at the equator or by increasing r_b in Mead's model for the magnetopause current. It appears that the theoretical model for the magnetopause current does not represent the observed fields at high latitudes. The theory does not include the polar cusp, which is an important feature observationally (Heikkila and Winningham, 1971; Frank, 1971; Fairfield and Ness, 1972). It is likely that the current system associated with the polar cusp substantially modifies the overall ΔB distribution at high latitudes including the polar cap magnetosphere.

Figure 8 gives curves representing the relation between the geocentric radial distances of the equatorial crossing of field lines and the dipole latitudes of their feet at the earth's surface, determined from the present model by field-line tracing in the noon and midnight meridians. Corresponding curves for the OGO 3 and 5 observations are also given in Figure 8; see Sugiura et al., 1971 for the details.

In spite of the discrepancies between the model and the observations described above, the general agreement in Figure 8 is remarkable, except for the outer magnetosphere at noon. It is cautioned, however, that the OGO results (broken lines in Fig. 8) are based on estimates from the observations and should still be considered as being provisional.

Several field lines traced in the noon and midnight meridian planes for the present model are shown in Figure 9. The field line leading to the neutral point in the noon meridian leaves the earth at a dipole latitude between 82° and 82.5°. As an example a field line leaving the earth's surface at 70° dipole latitude and at 0600 (or 1800) local time is traced in Figure 10; in the lower half of the figure, the projection of the field line onto the dipole equator is given, and in the top half, the field line is drawn on a curved surface containing it.

Olson (1972) has recently constructed a magnetospheric field model with distributed currents to represent the observed ΔB distribution. According to him, latitudinal cutoffs for low-energy cosmic rays determined from his model are in better agreement with recent satellite observations of cosmic rays than those calculated from earlier models. Details of his model are not available at this writing to enable us to make a comparison with the present model.

4. Conclusions

The magnetospheric field model presented above has an equatorial sheet current which is continuous from the tail to geocentric distances less than 3 R_E. This model represents the gross features of the ΔB distribution determined from the OGO 3 and 5 magnetic field observations

better than the existing models. The general agreement between the model and the observations warrants further improvements of the model by replacing the artificial disk current by a current system based on an appropriate particle distribution. Since the observational data on the particles responsible for the equatorial sheet current are not adequate, the discussions presented in the preceding section will be useful in selecting particle distributions for future models.

REFERENCES

Fairfield, D. H., Average magnetic-field configuration of the outer magnetosphere, J. Geophys. Res., 73, 7329, 1968.

Fairfield, D. H., and N. F. Ness, Imp 5 magnetic-field observations in the high-latitude outer magnetosphere near the noon meridian, J. Geophys. Res., 77, 611, 1972.

Frank, L. A., Plasma in the earth's polar magnetosphere, J. Geophys. Res., 76, 5202, 1971.

Heikkila, W. J., and J. D. Winningham, Penetration of magnetosheath plasma to low altitudes through the dayside magnetospheric cusps, J. Geophys. Res., 76, 883, 1971.

Mead, G. D., Deformation of the geomagnetic field by the solar wind, J. Geophys. Res., 69, 1181, 1964.

Olson, W. P., The shape of the tilted magnetopause, J. Geophys. Res., 74, 5642, 1969.

Olson, W. P., Distributed magnetospheric currents and their magnetic effects, (abstract), EOS, Trans. Am. Geophys. Union, 53, 1089, 1972.

Schield, M. A., Pressure balance between solar wind and magnetosphere, J. Geophys. Res., 74, 1275, 1969.

Speiser, T. W., and N. F. Ness, The neutral sheet in the geomagnetic tail: Its motion, equivalent currents, and field line connection through it, J. Geophys. Res., 72, 131, 1967.

Sugiura, M., The ring current, in Critical Problems of Magnetospheric Physics, Proceedings of the Joint COSPAR/IAGA/URSI Symposium, Madrid, Spain, May 11-13, 1972, edited by E. R. Dyer, IUCSTP Secretariat, c/o National Academy of Sciences, Washington, D. C., p. 195, 1972a.

Sugiura, M., Equatorial current sheet in the magnetosphere, J. Geophys. Res., 77, 6093, 1972b.

Sugiura, M., B. G. Ledley, T. L. Skillman, and J. P.Heppner, Magnetospheric-field distortions observed by Ogo 3 and 5, J. Geophys. Res., 76, 7552, 1971.

Williams, D. J., and G. D. Mead, Nightside magnetosphere configuration as obtained from trapped electrons at 1100 kilometers, J. Geophys. Res., 70, 3017, 1965.

FIGURES

Figure 1. Schematic views of the tail current in geocentric solar geomagnetic coordinates.

Figure 2. ΔB contours in the noon-midnight meridian plane for Kp = 0-1. The broken lines at the inner and outer boundaries of the contour map indicate border lines beyond which data are not available or are presently not considered to be reliable due to uncertainties in the orbit accuracies. See Sugiura et al. (1971) for the details for the derivation of ΔB.

Figure 3. ΔB contours in the dawn-dusk meridian plane for Kp = 0-1. (See the caption for Fig. 2).

Figure 4. ΔB contours in the noon-midnight meridian plane for Kp = 2-3. (See the caption for Fig. 2).

Figure 5. ΔB contours in the dawn-dusk meridian plane for Kp = 2-3. (See the caption for Fig. 2).

Figure 6. ΔB contours in the noon-midnight meridian derived from the present model.

Figure 7. ΔB contours in the dawn-dusk meridian derived from the present model.

Figure 8. Relationship between the geocentric radial distances of the equatorial crossing of field lines and the dipole latitudes of their feet on the earth's surface.

Figure 9. Field lines for the present model in the noon-midnight meridian plane. Field lines are labeled by the dipole latitudes at which they leave the earth's surface.

Figure 10. A field line leaving the earth at dipole latitude 70^{o} and at 0600 or 1800 local dipole time: in a curved (meridian) surface containing the field line in the upper half, and the projection onto the equatorial plane in the lower half.

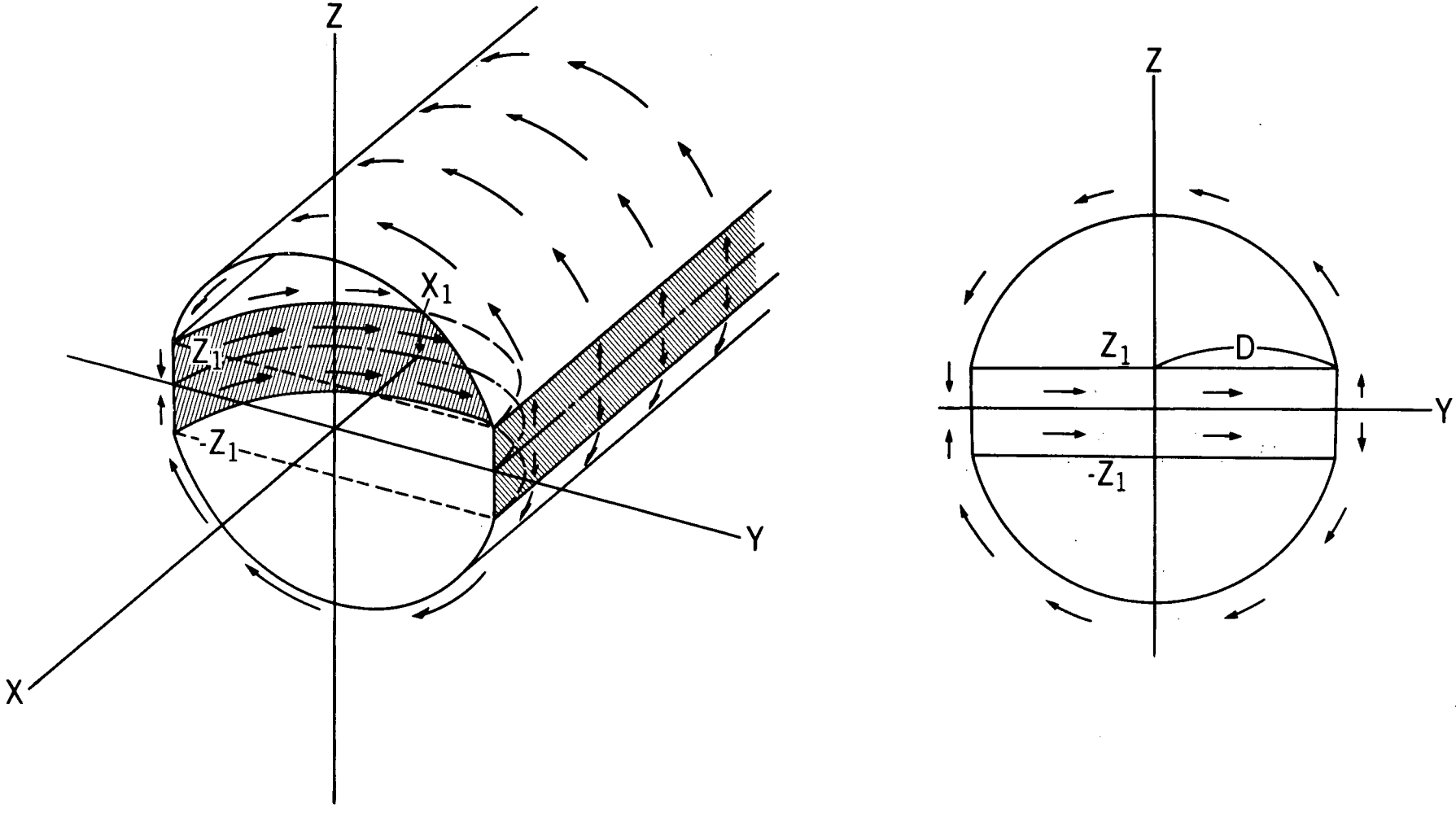

(a) SCHEMATIC VIEW OF THE TAIL CURRENT

(b) VIEW TOWARD THE -X AXIS

FIGURE 1

EQUAL ΔB CONTOURS (OGO 3 & 5 Rb MAGNETOMETER OBSERVATIONS)
ΔB = B (MEASURED) − B (REFERENCE FIELD)

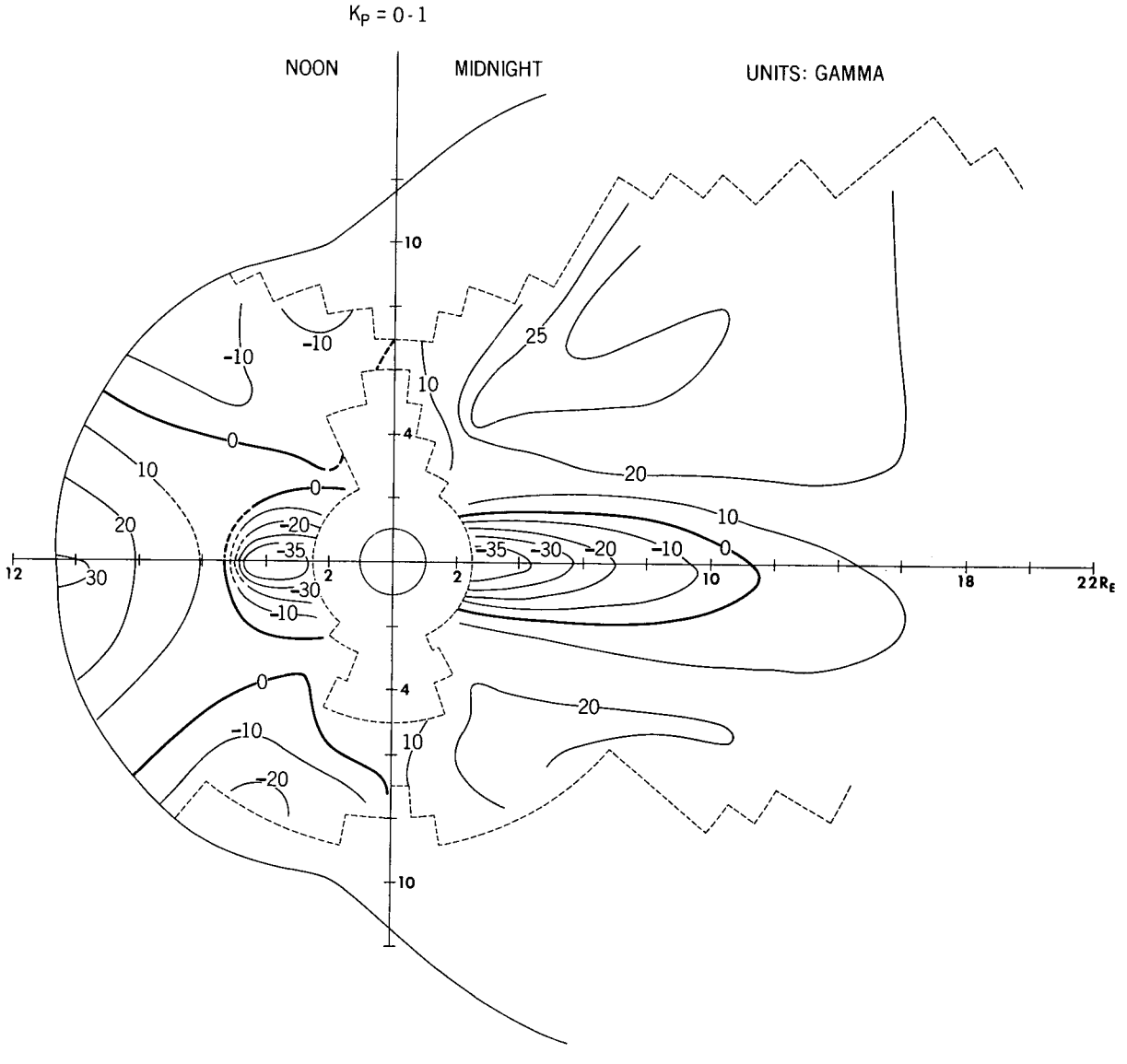

FIGURE 2

EQUAL ΔB CONTOURS (OGO 3 & 5 Rb MAGNETOMETER OBSERVATIONS)
ΔB=B (MEASURED) - B(REFERENCE FIELD)

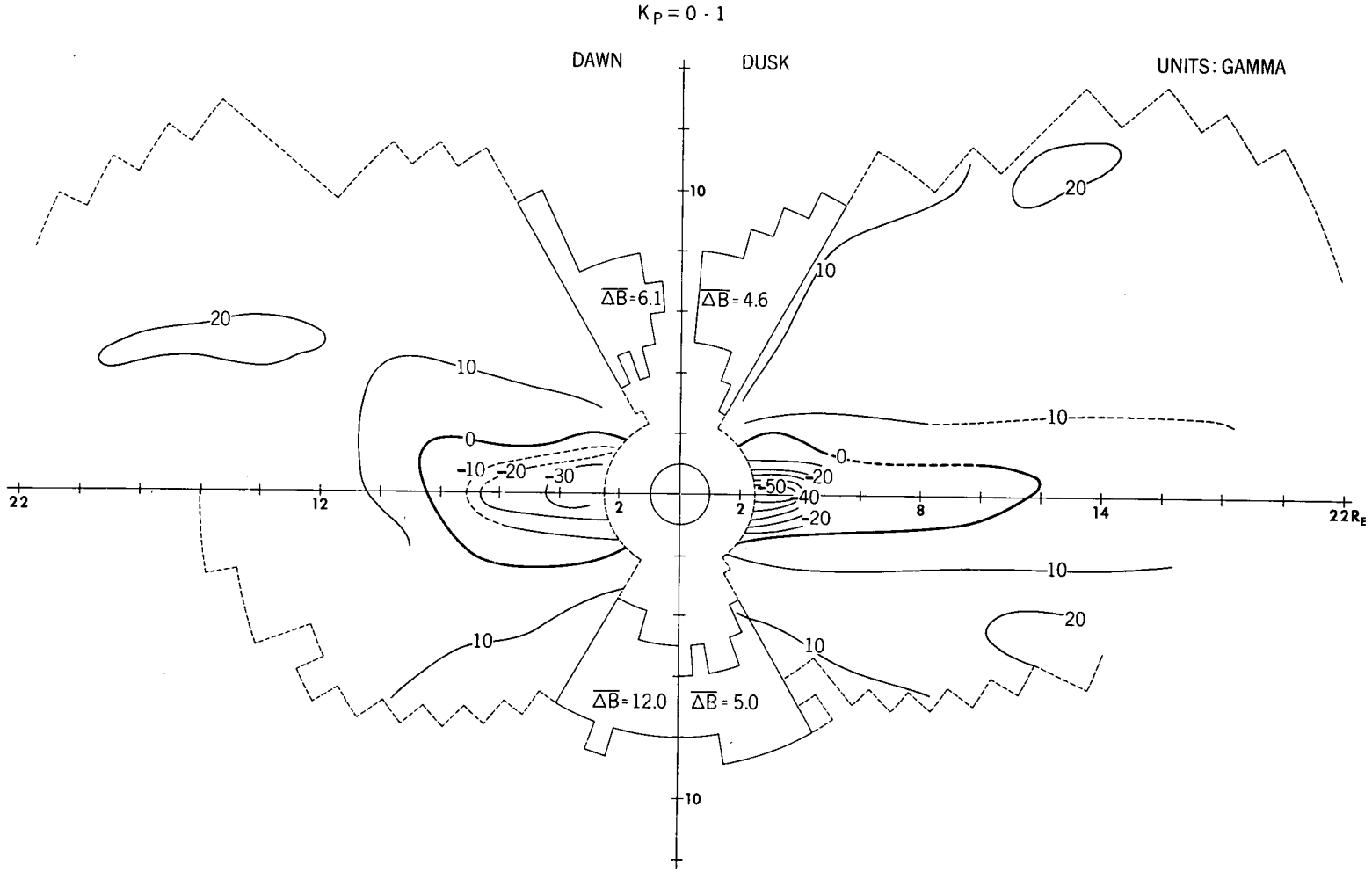

FIGURE 3

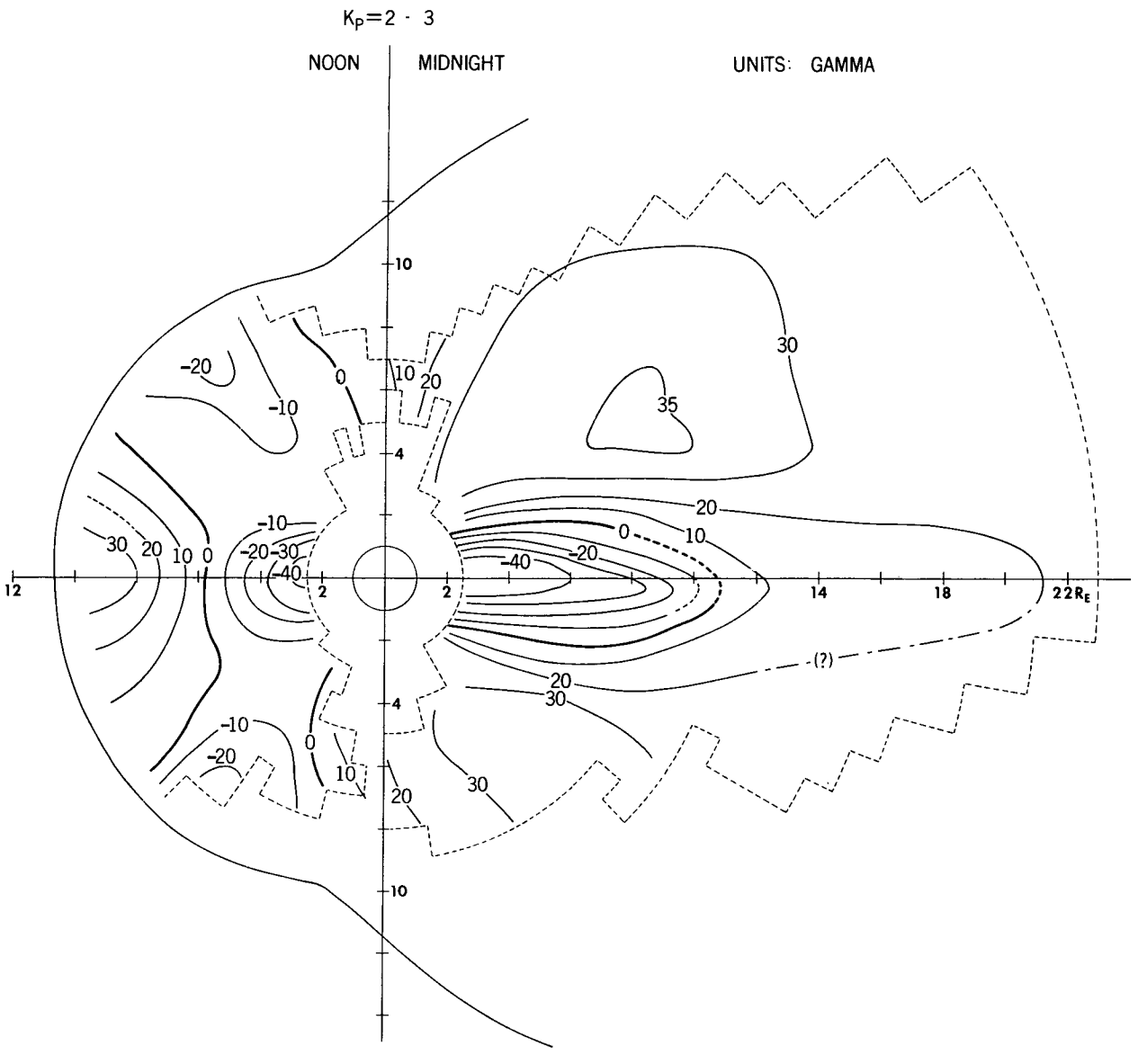
EQUAL ΔB CONTOURS (OGO 3&5 Rb MAGNETOMETER OBSERVATIONS)
ΔB=B (OBSERVED)−B(REFERENCE FIELD)
K_P=2 - 3
NOON
MIDNIGHT
UNITS: GAMMA
12
2
2
14
18
22R_E
10
4
4
10
-20
-10
0
10
20
30
35
-40
(?)

FIGURE 4

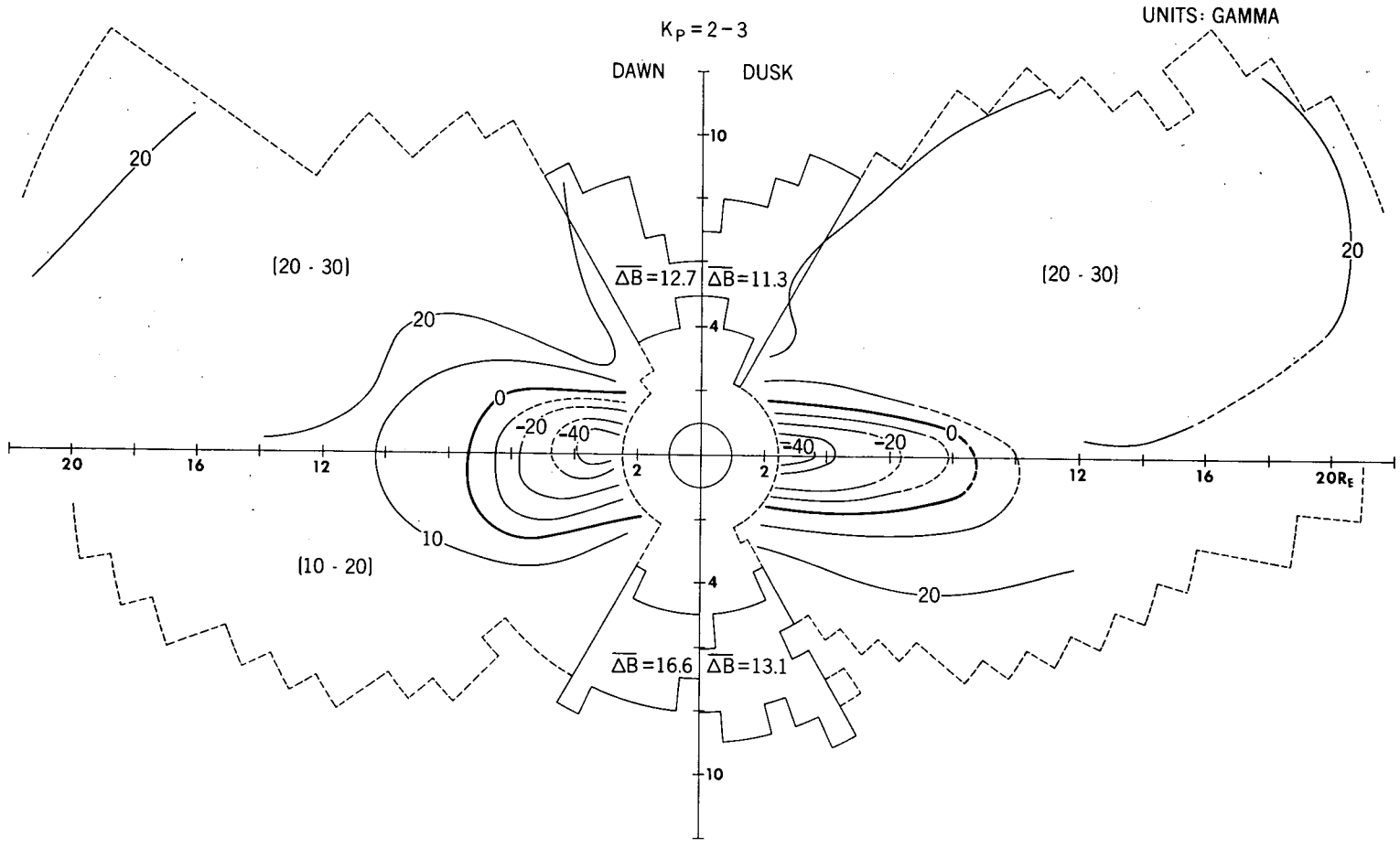
EQUAL ΔB CONTOURS (OGO 3 & 5 Rb MAGNETOMETER OBSERVATIONS)
ΔB = B (OBSERVED) – B(REFERENCE FIELD)
UNITS: GAMMA
$K_P = 2-3$
DAWN
DUSK
10
4
2
2
4
10
20
16
12
12
16
$20R_E$
20
20
0
-20
-40
-40
-20
0
20
10
20
[20 - 30]
[20 - 30]
[10 - 20]
$\overline{\Delta B}$=12.7
$\overline{\Delta B}$=11.3
$\overline{\Delta B}$=16.6
$\overline{\Delta B}$=13.1

FIGURE 5

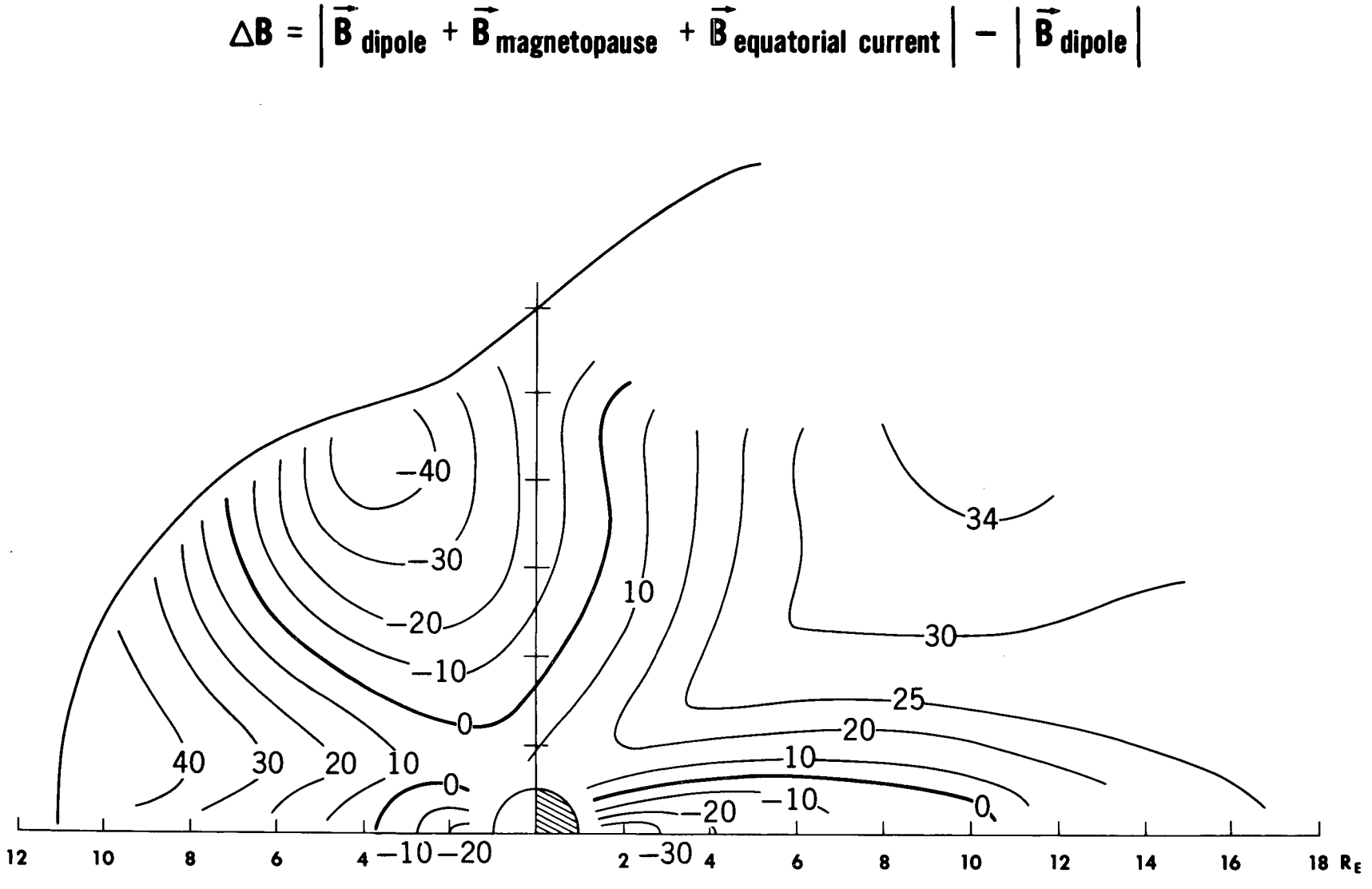
ΔB CONTOURS IN NOON–MIDNIGHT MERIDIAN
$\Delta B = \left| \vec{B}_{dipole} + \vec{B}_{magnetopause} + \vec{B}_{equatorial\ current} \right| - \left| \vec{B}_{dipole} \right|$
−40
−30
−20
−10
0
10
34
30
25
20
10
0
40
30
20
10
0
−20
−10
0
12
10
8
6
4
−10
−20
2
−30
4
6
8
10
12
14
16
18 R_E

FIGURE 6

ΔB CONTOURS IN DAWN-DUSK MERIDIAN

$$\Delta B = \left| \vec{B}_{\text{dipole}} + \vec{B}_{\text{magnetopause}} + \vec{B}_{\text{equatorial current}} \right| - \left| \vec{B}_{\text{dipole}} \right|$$

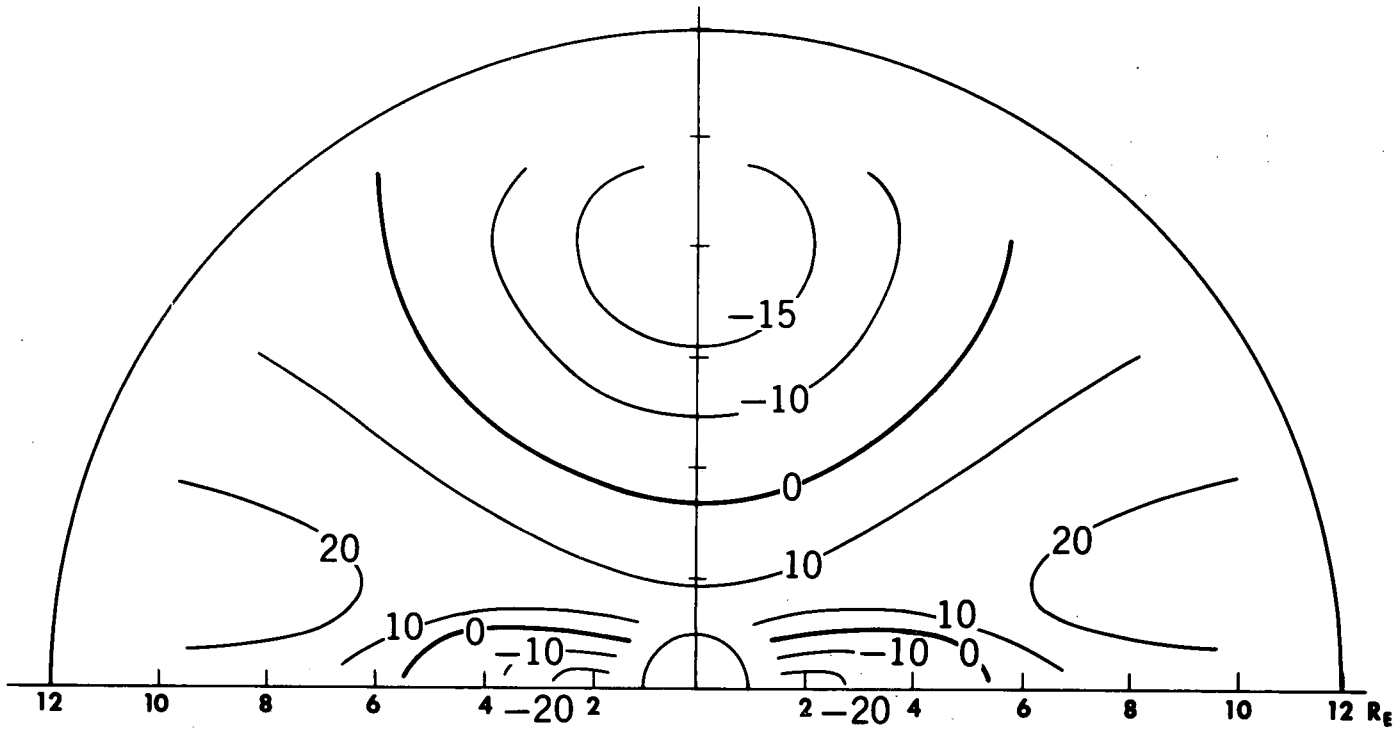

FIGURE 7

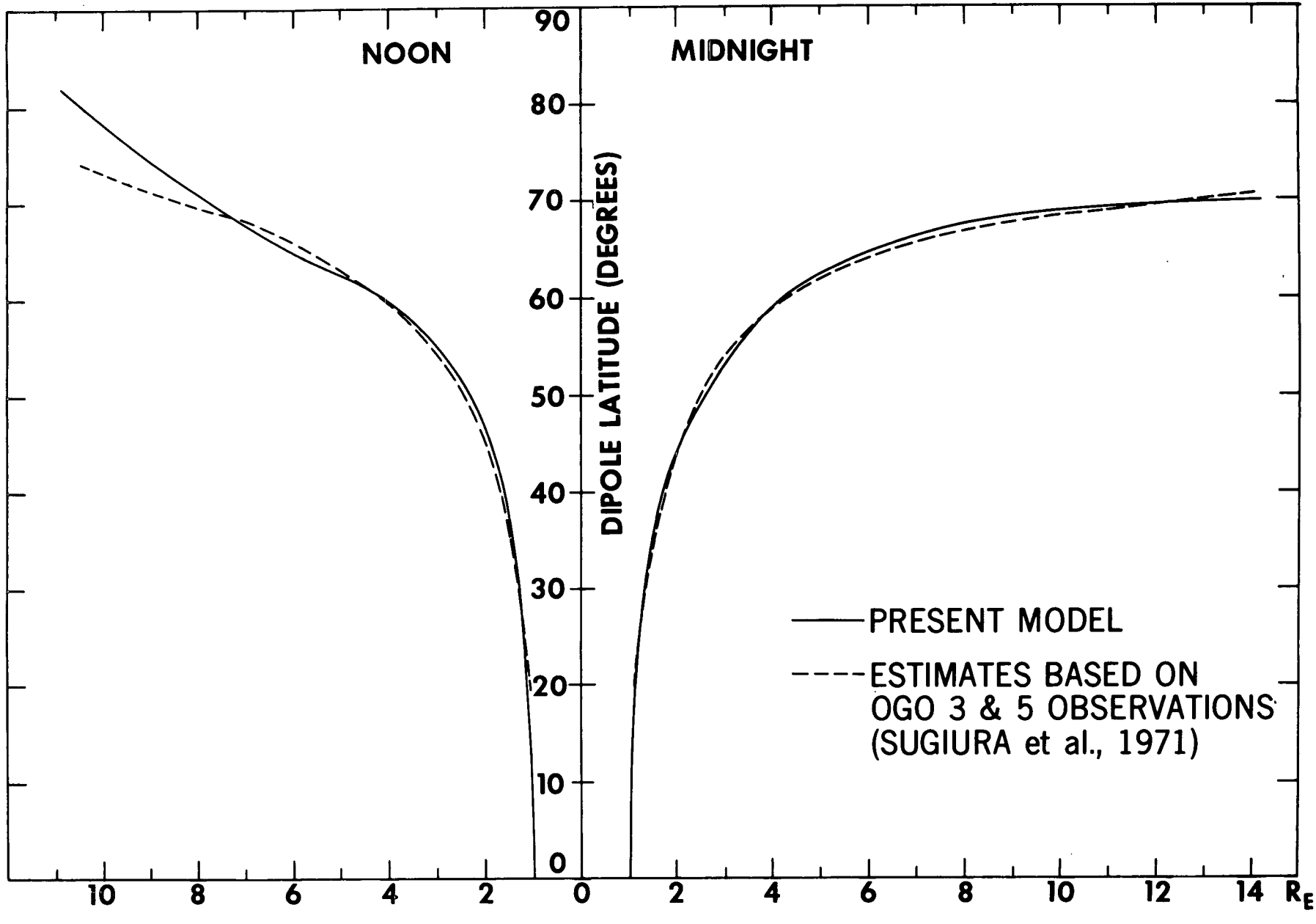
NOON
MIDNIGHT
DIPOLE LATITUDE (DEGREES)
90
80
70
60
50
40
30
20
10
0
10
8
6
4
2
0
2
4
6
8
10
12
14
R_E
PRESENT MODEL
ESTIMATES BASED ON OGO 3 & 5 OBSERVATIONS (SUGIURA et al., 1971)

FIGURE 8

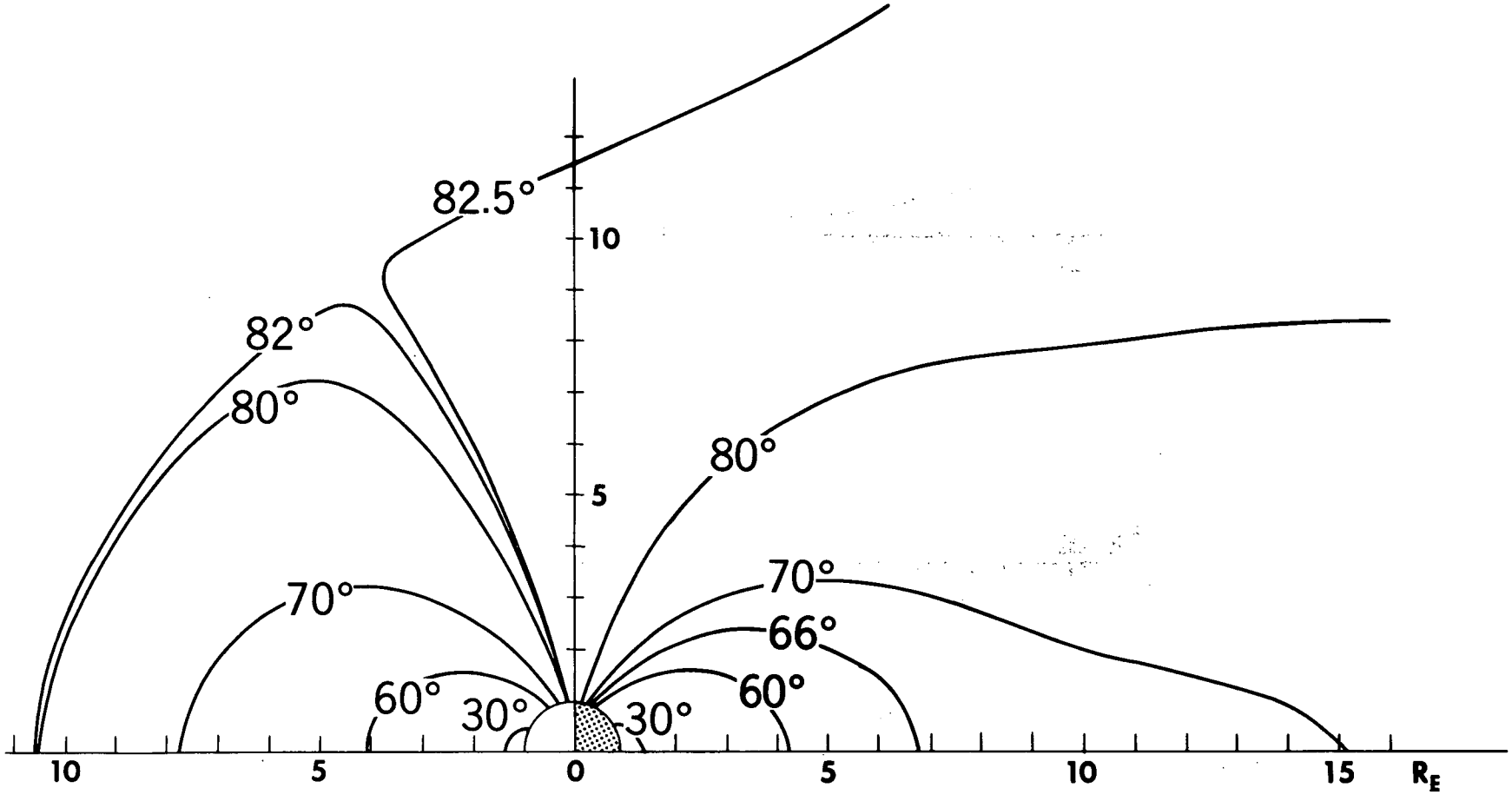

FIGURE 9

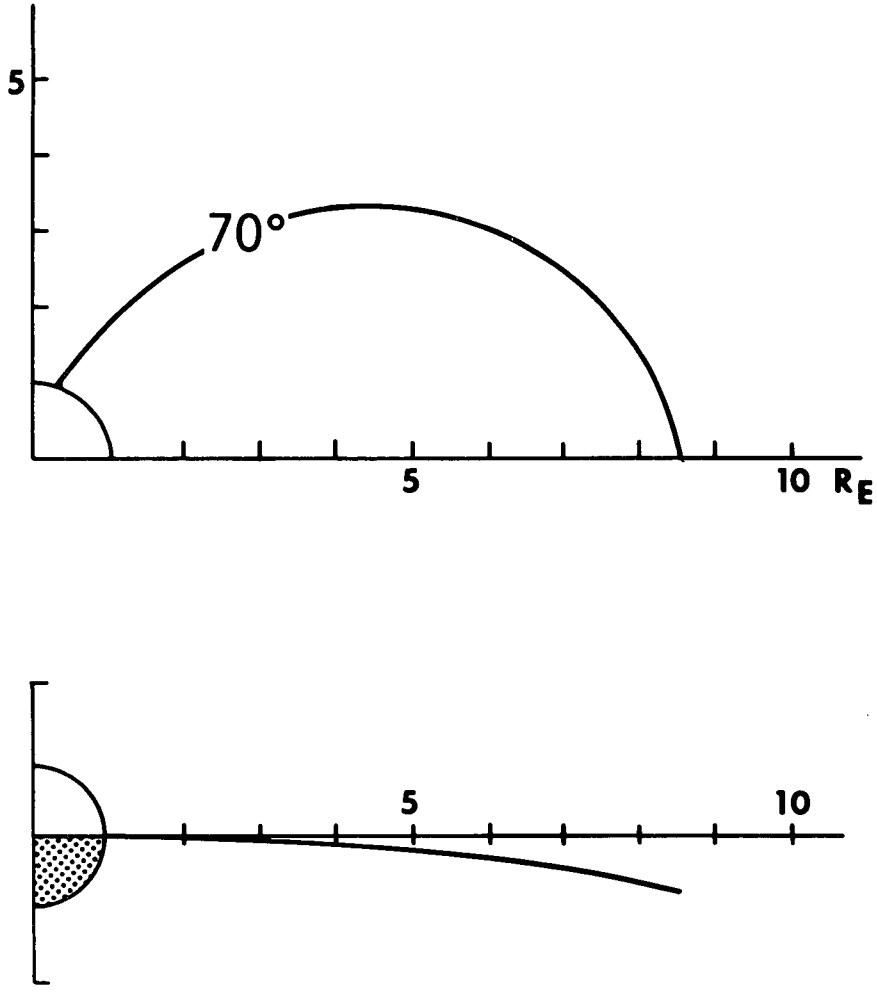

FIGURE 10